Inorganic Chemistry

Communication

pubs.acs.org/IC

Quantitative Fluorescent Detection of Pyrophosphate with Quinoline-Ligated Dinuclear Zinc Complexes

Yuji Mikata,*[†,‡] Anna Ugai,[‡] Risa Ohnishi,[‡] and Hideo Konno[§]

[†]*KYOUSEI* Science Center for Life and Nature and [‡]Department of Chemistry, Faculty of Science, Nara Women's University, Nara, Nara 630-8506, Japan

[§]National Institute of Advanced Industrial Science and Technology (AIST), 1-1-1 Higashi, Tsukuba, Ibaraki 305-8565, Japan

Supporting Information

ABSTRACT: Dinuclear zinc complex $[Zn_2(TQHPN)(AcO)]^{2+}$ exhibits characteristic fluorescence response (λ_{ex} = 317 nm and λ_{em} = 455 nm) toward pyrophosphate (PPi) with maximum fluorescence upon 1:1 Zn_2(TQHPN)−PPi complex formation. The crystallographic investigation utilizing P^1P^2−Ph_2PPi revealed that the fluorescent response mechanism is due to intramolecular excimer formation of two quinoline rings.

The development of anion recognition systems has become an important field of research. Phosphorus anions including pyrophosphate ($P_2O_7^{4-}$, PPi), adenosine triphosphate (ATP), and phosphorylated proteins and carbohydrates play many important roles in biology; thus, an accurate sensing system for such phosphorus anions could provide new insight to the phosphorylation process.[1,2] Fluorescent detection with chemical probes in the biological system is one of the ideal methodologies for anion sensing in solution because of its high sensitivity and high spatial resolution, as well as rapid response times. To be useful in a biological environment, fluorescence probes need high target specificity and applicability to quantitative analysis. The ability of the probe to quickly respond to concentration changes of the analyte would be ideal for real-time quantitative analysis.[3,4]

PPi-specific fluorescent probes have been exploited in recent decades,[1,2,5−17] and many of these sensing molecules contain a dinuclear metal core for substrate binding interactions. In this Communication, pyrophosphate-induced fluorescence changes of a dinuclear zinc complex supported by quinoline-based ligands, *N*,*N*,*N*′,*N*′-tetrakis(2-quinolylmethyl)-2-hydroxy-1,3-propanediamine (HTQHPN; Figure 1a),[18] have been investigated. This metalloligand generates a fluorescent 1:1 complex with PPi (ϕ = 0.029) via intramolecular excimer formation.

The HTQHPN ligand afforded a dinuclear zinc complex upon mixing with 2 equiv of $Zn(AcO)_2$ (Figures S1 and S2 in the Supporting Information, SI). Figure 1b shows the crystal structure of the acetate-bridged complex $[Zn_2(TQHPN)(OAc)](ClO_4)_2$ [**1**·$(ClO_4)_2$]. Both zinc centers are pentacoordinate, exhibiting slightly distorted trigonal-bipyramidal geometries (τ = 0.81 for Zn1 and 0.88 for Zn2).[19] The dizinc complex **1** in an aqueous *N*,*N*-dimethylformamide (DMF) solution (1:1 DMF/H_2O) exhibited weak fluorescence upon excitation at 317 nm, but with the addition of PPi to this solution, fluorescence enhancement was observed (Figure 2). The fluorescence intensity at 455 nm in the presence of 1 equiv of

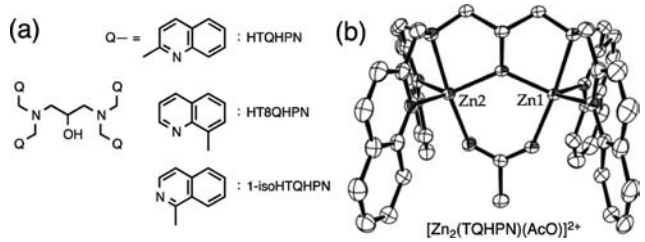

Figure 1. (a) Structures of the ligands. (b) ORTEP plot for **1**·$(ClO_4)_2$·$2CH_3CN$ in 50% probability. Atoms of counteranions, hydrogens, and solvents were omitted for clarity.

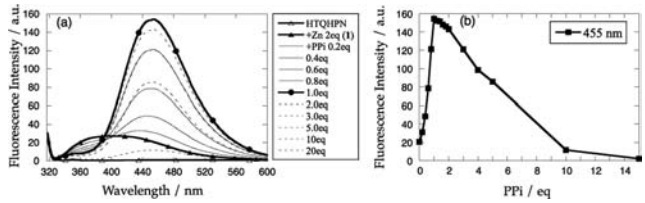

Figure 2. (a) Fluorescence spectra for 34 μM **1** in DMF/H_2O (1:1) in the presence of increasing amounts of PPi ranging from 0 to 680 μM concentration at 25 °C (λ_{ex} = 317 nm). (b) Plot of the fluorescence intensity change at 455 nm.

PPi was enhanced 8-fold in comparison to **1** in the absence of PPi. The addition of further equivalents of PPi to the zinc dimer complex in solution leads to a decrease in the fluorescence intensity (Figure 2b). In the presence of 15 equiv of PPi, fluorescence completely disappears and UV−vis spectra shown in Figure S3 in the SI reveal that free HTQHPN was formed by the removal of zinc by excess PPi.[20,21] This was also confirmed by electrospray ionization mass spectrometry measurement (Figure S40 in the SI). Large excess of PPi increased the pH of the solution, but this is not the reason for decomplexation of Zn_2(TQHPN)−PPi because a parallel experiment employing a buffer solution with constant pH (pH = 7.5) gave similar results (Figure S42 in the SI).

The fluorescence enhancement is specific to PPi because a much smaller response was observed for ATP (50% of PPi) and adenosine diphosphate (30% of PPi) in the presence of 1 equiv of the anion (Figures 3 and S4 in the SI). Other anions including monophosphates (AMP and PO_4^{3-}) did not induce any

Received: June 25, 2013
Published: August 28, 2013

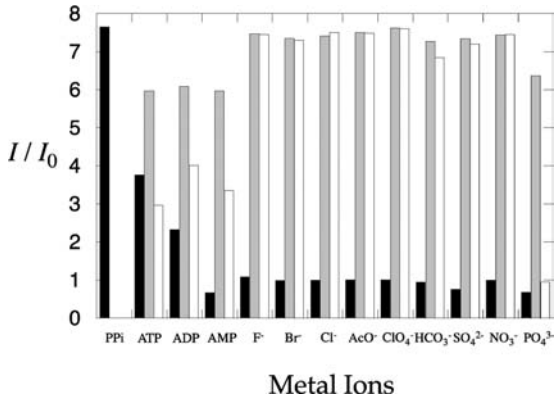

Figure 3. Plot of the fluorescence intensity of a 34 μM Zn_2(TQHPN) complex (**1**) at 455 nm (λ_{ex} = 317 nm) in DMF/H_2O (1:1) at 25 °C in the presence of 1 equiv of anions (filled bars), 1 equiv of anion + 1 equiv of PPi (gray bars), and 1 equiv of PPi + 10 equiv of anion (open bars).

fluorescence enhancement. Importantly, this fluorescent PPi sensing is valid even in the presence of other anions (1 equiv), indicating the preferred binding of PPi over other anions including other phosphate species. However, a further addition of excess (10 equiv) phosphate species results in considerable fluorescence quenching because of the removal of zinc from the ternary complex (Figure S41 in the SI). The fluorescence of Zn_2(TQHPN)−PPi was not perturbed by 10 equiv of non-phosphate anions.

In many cases, fluorescent PPi sensing was achieved by intermolecular excimer formation between two chromophores[6,13,15] or electrostatic perturbation of metal center(s)[9−11] upon PPi binding. However, there are very few examples in which the spectroscopic response mechanism was discussed based on structural analysis by X-ray crystallography.[9,16]

All crystallization trials for the Zn_2(TQHPN)−PPi complex resulted in free ligand HTQHPN formation. Using the diphenyl ester of PPi, P^1P^2−diphenyl pyrophosphate (Ph_2PPi),[22] as a crystallizable substitute of PPi was successful. Fluorescence enhancement of the Zn_2(TQHPN) complex in the long-wavelength region (433 nm) was also induced by Ph_2PPi, and in parallel, the monophenyl phosphate ($PhOPO_3^{2-}$) exhibited similar weak fluorescence spectral changes in comparison to PO_4^{3-} (Figure S5 in the SI).

Having confirmed that phenyl esters can be used as an alternative for inorganic phosphate species in this work, the crystal structure analyses for complexes of Zn_2(TQHPN)−Ph_2PPi (**2**) and Zn_2(TQHPN)−$PhOPO_3^{2-}$ (**3**) were investigated (Figure 4). For complex **2**, both zinc centers adopt a hexacoordinate geometry ligated by three nitrogen atom and an μ-alkoxo oxygen atom from TQHPN, a bridging phosphate oxygen atom, and an oxygen atom from water or pyrophosphate (Figure 4a). As a result of Ph_2PPi binding, two quinoline groups opposite to the PPi side are forced into a close parallel arrangement that is suitable for enhancing excimer emission at a lower-energy region. This is the first crystal structure in which PPi-induced excimer arrangement of the probe(s) is clearly shown. On the other hand, both zinc centers in the monophosphate complex **3** were of pentacoordinate geometry because of the lack of an extra phosphate moiety in comparison with the diphosphate PPi (Figure 4b). This distorted trigonal-bipyramidal dizinc center (τ = 0.61 for Zn1 and 0.78 for Zn2) of **3** allows for an extended structure for all quinolines with limited quinoline

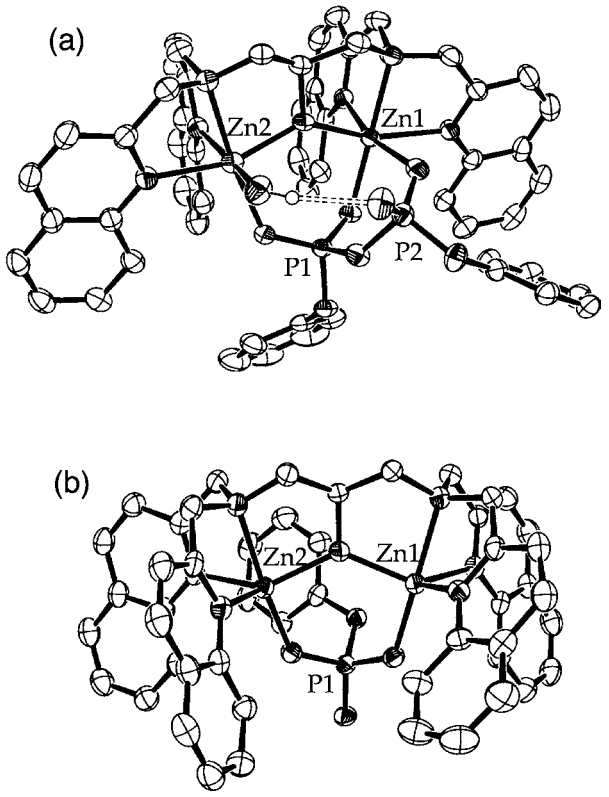

Figure 4. ORTEP plot for (a) **2**·ClO_4·2THF·1.5H_2O and (b) **3**·ClO_4·THF·6H_2O in 50% probability. Atoms of counteranions, hydrogens, and solvents were omitted for clarity.

intramolecular interactions similar to acetate-bridged complex **1**. Figure S6 in the SI highlights the difference in interquinoline interaction of the Ph_2PPi complex **2** in comparison to the acetate or monophosphate complexes **1** and **3** in the crystal structures.

Analogous excimer formation induced by PPi binding was observed in the *N*,*N*,*N*′,*N*′-tetrakis(8-quinolylmethyl)-2-hydroxy-1,3-propanediamine (HT8QHPN; Figure 1a) system **4** (Figures S7−S9 and S12a in the SI). In this case, the dizinc center of **4** was hexa- and pentacoordinate with P^1P^2 ligation by Ph_2PPi, missing the H_2O ligand bound to Zn2 found in complex **2**. In contrast, for the *N*,*N*,*N*′,*N*′-tetrakis(1-isoquinolylmethyl)-2-hydroxy-1,3-propanediamine (1-isoHTQHPN; Figure 1a) complex **5**, neither fluorescence enhancement nor excimer formation in the crystal structure was observed (Figures S10−S11 and S12b in the SI), likely because PPi binding does not promote close interisoquinoline interaction, as observed in the crystal structure. P^1P^2 oxygen chelation to a zinc center of the metalloligand is indispensable for the excimer formation observed in the Zn_2(TQHPN) system.

A titration experiment of a PPi solution with **1** to determine the concentration of PPi was conducted (Figures 5 and S13 in the SI). Maximum fluorescence was achieved at [**1**] = [PPi], and then excess **1** quenched the fluorescence probably because of formation of the $[Zn_2(TQHPN)]_2$−PPi species, in which the quinoline excimer structure was collapsed by the monophosphate-like binding of PPi to each dizinc unit. As seen in Figure 5, a very sharp titration curve suitable for determination of the concentration of a PPi solution was obtained because of self-quenching of Zn_2(TQHPN) at a late stage of the titration (Figure S43 in the SI).

dx.doi.org/10.1021/ic401605m | *Inorg. Chem.* 2013, 52, 10223−10225

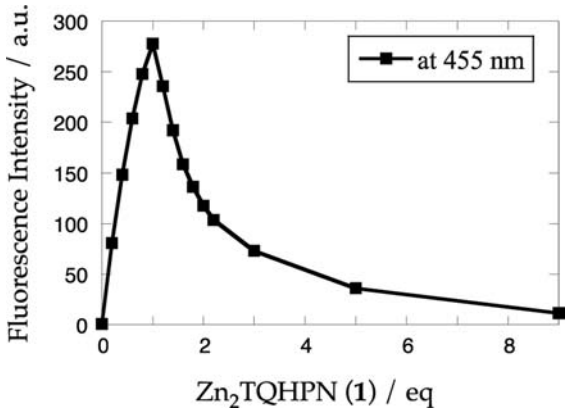

Figure 5. Fluorescent titration of a PPi solution (34 μM, 3 mL in 1:1 DMF/H_2O) at 455 nm with **1** (5 mM DMF) at 25 °C (λ_{ex} = 317 nm).

The effect of the pH was found to be limited in the range of pH = 4−9 (Figure S14 in the SI). The dizinc complex is unstable at lower and higher pH because of zinc release by protonation of the ligand and formation of $Zn(OH)_2$, respectively, resulting in decreased fluorescence.

In summary, the dinuclear zinc complex **1** exhibits a characteristic fluorescence response toward pyrophosphate PPi with OFF−ON−OFF-type fluorescence intensity changes, which allows quantitative fluorescence determination of the PPi concentration. The crystallographic investigation utilizing Ph_2PPi and $PhOPO_3^{2-}$ revealed that the fluorescence enhancement mechanism of **1** is due to intramolecular excimer formation by the second phosphate coordination to the zinc center. This is the first crystal structure of PPi-induced excimer arrangement revealed in the solid state. The present results and crystallographic analysis technique utilizing phenyl phosphate species could lead to an improved molecular design for new fluorescent probes with high target specificity and a new response mechanism for phosphate-related analytes.

■ ASSOCIATED CONTENT

Ⓢ Supporting Information

Experimental procedure for synthesis and titration experiment, Tables S1 and S2, Figures S1−S43, and crystallographic data in CIF format. This material is available free of charge via the Internet at http://pubs.acs.org.

■ AUTHOR INFORMATION

Corresponding Author

*E-mail: mikata@cc.nara-wu.ac.jp.

Notes

The authors declare no competing financial interest.

■ ACKNOWLEDGMENTS

The authors thank Prof. Tim Storr and John Thompson of Simon Fraser University for their helpful discussion about X-ray crystallography. This work was supported by the Research for Promoting Technological Seeds, JST, Adaptable and Seamless Technology Transfer Program through Target-driven R&D, JST, Grant-in Aid for Scientific Research from the MEXT, Japan, and the Nara Women's University Intramural Grant for Project Research.

■ REFERENCES

(1) Spangler, C.; Schaeferling, M.; Wolfbeis, O. S. *Microchim. Acta* **2008**, *161*, 1−39.
(2) Kim, S. K.; Lee, D. H.; Hong, J.-I.; Yoon, J. *Acc. Chem. Res.* **2009**, *42*, 23−31.
(3) Zhang, X.-a.; Hayes, D.; Smith, S. J.; Friedle, S.; Lippard, S. J. *J. Am. Chem. Soc.* **2008**, *130*, 15788−15789.
(4) Buccella, D.; Horowitz, J. A.; Lippard, S. J. *J. Am. Chem. Soc.* **2011**, *133*, 4101−4114.
(5) Vance, D. H.; Czarnik, A. W. *J. Am. Chem. Soc.* **1994**, *116*, 9397−9398.
(6) Nishizawa, S.; Kato, Y.; Teramae, N. *J. Am. Chem. Soc.* **1999**, *121*, 9463−9464.
(7) Gunnlaugsson, T.; Davis, A. P.; O'Brien, J. E.; Glynn, M. *Org. Lett.* **2002**, *4*, 2449−2452.
(8) Fabbrizzi, L.; Marcotte, N.; Stomeo, F.; Taglietti, A. *Angew. Chem., Int. Ed.* **2002**, *41*, 3811−3814.
(9) Lee, D. H.; Im, J. H.; Son, S. U.; Chung, Y. K.; Hong, J.-I. *J. Am. Chem. Soc.* **2003**, *125*, 7752−7753.
(10) Lee, D. H.; Kim, S. Y.; Hong, J.-I. *Angew. Chem., Int. Ed.* **2004**, *43*, 4777−4780.
(11) Jang, Y. J.; Jun, E. J.; Lee, Y. J.; Kim, Y. S.; Kim, J. S.; Yoon, J. *J. Org. Chem.* **2005**, *70*, 9603−9606.
(12) Gunnlaugsson, T.; Davis, A. P.; O'Brien, J. E.; Glynn, M. *Org. Biomol. Chem.* **2005**, *3*, 48−56.
(13) Cho, H. K.; Lee, D. H.; Hong, J.-I. *Chem. Commun.* **2005**, 1690−1692.
(14) Kim, S. K.; Singh, N. J.; Kwon, J.; Hwang, I.-C.; Park, S. J.; Kim, K. S.; Yoon, J. *Tetrahedron* **2006**, *62*, 6065−6072.
(15) Lee, H. N.; Xu, Z.; Kim, S. K.; Swamy, K. M. K.; Kim, Y.; Kim, S.-J.; Yoon, J. *J. Am. Chem. Soc.* **2007**, *129*, 3828−3829.
(16) Lee, J. H.; Park, J.; Lah, M. S.; Chin, J.; Hong, J.-I. *Org. Lett.* **2007**, *9*, 3729−3731.
(17) Chen, W.-H.; Xing, Y.; Pang, Y. *Org. Lett.* **2011**, *13*, 1362−1365.
(18) Mikata, Y.; Wakamatsu, M.; So, H.; Abe, Y.; Mikuriya, M.; Fukui, K.; Yano, S. *Inorg. Chem.* **2005**, *44*, 7268−7270.
(19) Addison, A. W.; Rao, T. N.; Reedijk, J.; van Rijn, J.; Verschoor, G. C. *J. Chem. Soc., Dalton Trans.* **1984**, 1349−1356.
(20) Pathak, R. K.; Tabbasum, K.; Rai, A.; Panda, D.; Rao, C. P. *Anal. Chem.* **2012**, *84*, 5117−5123.
(21) Pathak, R. K.; Hinge, V. K.; Rai, A.; Panda, D.; Rao, C. P. *Inorg. Chem.* **2012**, *51*, 4994−5005.
(22) Ruveda, M. A.; Zerba, E. N.; de Moutier Aldao, E. M. *Tetrahedron* **1972**, *28*, 5011−5016.